

Hot-pressing process modeling for medium density fiberboard (MDF) Technical Report 1 .

Noberto Nigro and Mario Storti
Centro Internacional de Métodos Computacionales en Ingeniería
<http://minerva.unl.edu.ar/gtm-eng.html>

October 30, 2024

\$Id: hotpress.tex,v 1.6 1999/06/17 15:39:19 mstorti Exp \$

Abstract

In this paper we present a numerical solution for the mathematical modeling of the hot-pressing process applied to medium density fiberboard. We have started our development from the paper of Carvalho & Costa [2] and the model presented by Humphrey in his PhD. thesis [4] with some modifications and extensions in order to take into account mainly the convective effects on the phase change term and also a conservative numerical treatment of the resulting system of partial differential equations.

Contents

1	Hot-pressing mathematical model	2
1.1	Multiphase model	2
1.2	Energy balance	3
1.3	Steam mass balance	3
1.4	Gas mixture mass balance	4
2	Summary of equations and boundary conditions	5
3	Numerical method	5
4	Physical and transport properties	7
4.1	Thermal conductivity	7
4.1.1	Density correction	7
4.1.2	Moisture correction	7
4.1.3	Temperature correction	7
4.1.4	Heat flux direction correction	8
4.2	Permeability	8
4.2.1	Variation of vertical permeability with board material density	9

4.2.2	Horizontal permeability	10
4.3	Vapour Density	10
4.4	Saturated vapour pressure	10
4.5	Latent heat of evaporation and heat of wetting	10
4.6	Specific heat of mattress material	11
4.7	Porosity	11
5	Numerical results	11
5.1	Original numerical experiment	13
5.2	Further numerical experiments	18
6	Appendix. Derivation of the averaged energy balance equation	19

1 Hot-pressing mathematical model

Following the Carvalho & Costa paper [2] the following dimensionless numbers and reference values appear:

$$\text{Fo}_z = \frac{1}{\rho_s} \quad (1)$$

$$\text{Fo}_{mz} = \epsilon \quad (2)$$

$$\rho_{v0} = \frac{\text{MM}_w}{R} \quad (3)$$

$$N_{pz} = \frac{1}{\epsilon} \quad (4)$$

$$\text{Pe}_z = 1 \quad (5)$$

$$\text{Pe}_{mz} = \frac{1}{\epsilon} \quad (6)$$

$$\rho_0 = \frac{\text{MM}_a}{R} \quad (7)$$

$$\rho_{v0} = \frac{\text{MM}_w}{R} \quad (8)$$

where ρ_s is the solid material density, ϵ represents the material porosity, MM_w, MM_a are the water and air molecular weight in $Kg/Kmol$ and R is the particular gas constant for air ($R = 8314 K J/(KmolK)$). $\text{Fo}_z, \text{Fo}_{mz}$ are the thermal and mass Fourier number, ρ_0, ρ_{v0} are reference values for air and vapor density, N_{pz} is the number of voids in a unit volume, $\text{Pe}_z, \text{Pe}_{mz}$ are the thermal and mass Peclet values representing the relative importance of convective effects in the transport equations. In order to match our dimensional form with the dimensionless set of equations presented in the Carvalho & Costa paper [2] we have adopted a unit value for $T_0 - T_\infty, \tau, L_{x,y,z}$.

1.1 Multiphase model

In order to avoid modeling the material down to the scale of the microstructure (the fibers in this case), non homogeneous materials are solved via “averaged equations” so that the intrincated microstructure

results in a continuum with averaged properties. This averaged equations and properties can be deduced in a rigorous way through the theory of mixtures and averaging operators[14].

We will not enter in the details of all the derivations, but will derive the averaged energy balance equation.

1.2 Energy balance

$$\rho_s C_p \frac{\partial T}{\partial t} = \nabla \cdot (k \nabla T - \rho_v \mathbf{v}_g (C_{pv} T + \lambda)) - \dot{m}(\lambda + Q_l) \quad (9)$$

The main difference between this equation and that presented by both Carvalho & Costa [2] and Humphrey [4] is in the addition of the water evaporation heat in the convection term instead of considering the phase change effect only on the temporal term. This term should be included because both phases, the solid material and the vapor are in relative motion and we think that its influence is not negligible in a high temperature process.

1.3 Steam mass balance

Carvalho & Costa [2] have proposed the following steam mass conservation equation:

$$\dot{m} = \frac{MM_w}{R} \epsilon \nabla \cdot \left[-D_v \nabla \left(\frac{P_v}{T} \right) + \frac{1}{\epsilon} \mathbf{v}_g \frac{P_v}{T} \right] \quad (10)$$

Considering that the steam is treated as an ideal gas

$$\frac{P_v}{T} = MM_w^{-1} R \rho_v \quad (11)$$

so, the resulting mass balance for the steam may be written as:

$$\dot{m} = \nabla \cdot [-\epsilon D_v \nabla \rho_v + \mathbf{v}_g \rho_v] \quad (12)$$

We prefer to adopt this kind of expression instead of 10 because it is written in a conservative form that is more agreeable for a numerical treatment. The left hand side term represent the mass interfacial transport and those in the right hand side take into account the mass diffusion and the mass convection. However, it should be noted that this last expression does not have a temporal term like in every consistent balance equation. For example, if no evaporation is considered the 12 is only valid for a static situation that it is not the general case. Then, we rewrite the steam mass balance as:

$$\epsilon \frac{\partial \rho_v}{\partial t} = \nabla \cdot [\epsilon D_v \nabla \rho_v - \mathbf{v}_g \rho_v] + \dot{m} \quad (13)$$

This is another difference between our model and that proposed by Carvalho & Costa [2].

1.4 Gas mixture mass balance

Finally, because the gas phase is composed by two main constituents, the steam and the air we may use an additional equation for the mass transport of the whole gas phase.

$$\frac{\partial P}{\partial t} = -\frac{1}{\epsilon} \nabla \cdot \left(-\frac{K_g}{\mu} \frac{P}{T} \nabla P \right) T + \frac{\dot{m}}{\epsilon M M_a} T R + \frac{P}{T} \frac{\partial T}{\partial t} \quad (14)$$

Again, assuming the ideal gas law as state equation for this phase,

$$\frac{\partial}{\partial t} \left(\frac{P}{T} \right) = -\frac{1}{\epsilon} \nabla \cdot \left(-\frac{K_g}{\mu} \rho_g \nabla P \right) + \frac{\dot{m} R}{\epsilon M M_a} \quad (15)$$

finally we arrive to the following expression:

$$\epsilon \frac{\partial \rho_g}{\partial t} = -\nabla \cdot (\rho_g \mathbf{v}_g) + \dot{m} \quad (16)$$

In order to close the system of equations we need to introduce a relationship between \dot{m} and $\frac{\partial P_v}{\partial t}$. Here, we have proposed the following strategy to avoid the definition of this relationship. We consider the steam mass balance above presented (13) and we have proposed an additional equation for the total water content H of the following form:

$$\rho_s H = \epsilon \rho_v + \rho_L \quad (17)$$

where ρ_L is the bound water density (= bound water per unit volume). The bound water only may be transferred to the gas phase (solid to steam) assuming that no liquid phase is considered. So,

$$\dot{m} = -\frac{\partial \rho_L}{\partial t} \quad (18)$$

and then

$$\rho_s \frac{\partial H}{\partial t} = \epsilon \frac{\partial \rho_v}{\partial t} + \frac{\partial \rho_L}{\partial t} \quad (19)$$

$$= \nabla \cdot [\epsilon D_v \nabla \rho_v - \mathbf{v}_g \rho_v] \quad (20)$$

Air mass balance equation arises subtracting (13) from (16)

$$\epsilon \frac{\partial \rho_a}{\partial t} = \nabla \cdot [-\epsilon D_v \nabla \rho_v - \mathbf{v}_g \rho_a] \quad (21)$$

Due to the fact that the mean macroscopic diffusive fluxes should be null

$$D_v \nabla \rho_v + D_a \nabla \rho_a = 0 \quad (22)$$

the air mass balance is transformed in:

$$\epsilon \frac{\partial \rho_a}{\partial t} = \nabla \cdot [\epsilon D_a \nabla \rho_a - \mathbf{v}_g \rho_a] \quad (23)$$

expression very similar to (13) but here valid for the air. As it is obvious for the air transport there is no evaporation.

2 Summary of equations and boundary conditions

In order to clarify the mathematical model that is finally used for the simulation of hot-pressing process we present the following brief summary of partial differential equations.

$$\rho_s C_p \frac{\partial T}{\partial t} = \nabla \cdot (k \nabla T - \rho_v \mathbf{v}_g (C_{pv} T + \lambda)) - \dot{m}(\lambda + Q_l) \quad (24)$$

$$\rho_s \frac{\partial H}{\partial t} = \nabla \cdot [\epsilon D_v \nabla \rho_v - \mathbf{v}_g \rho_v] \quad (25)$$

$$\epsilon \frac{\partial \rho_a}{\partial t} = \nabla \cdot [\epsilon D_a \nabla \rho_a - \mathbf{v}_g \rho_a] \quad (26)$$

The boundary conditions are the following:

- At the press platen:

$$T = T_{\text{platen}} \quad (27)$$

$$\mathbf{v}_g = 0, \quad \frac{\partial \rho_a}{\partial z} = 0, \quad \frac{\partial \rho_v}{\partial z} = 0 \quad (28)$$

- At the center line ($r = 0$):

$$\frac{\partial T}{\partial r} = 0, \quad \frac{\partial H}{\partial r} = 0, \quad \frac{\partial \rho_a}{\partial r} = 0 \quad (29)$$

- At the mid plane ($z = 0$):

$$\frac{\partial T}{\partial z} = 0, \quad \frac{\partial H}{\partial z} = 0, \quad \frac{\partial \rho_a}{\partial z} = 0 \quad (30)$$

- At the exit boundary ($r = R_{\text{ext}}$):

$$\frac{\partial T}{\partial r} = 0, \quad \text{null diffusive heat flux} \quad (31)$$

$$P_v = P_{v,\text{atm}} \quad (32)$$

$$P_a = P_{a,\text{atm}} \quad (33)$$

3 Numerical method

The above system of equations contains three main unknowns, the temperature, the moisture content and the air density representing the dependent variables of the problem also called the state variable. In this work we have used as independent variables the time and three spatial coordinates. Due to the physical and geometrical inherent complexity of this problem this may be computed only by numerical methods. For the spatial discretization we have employed finite elements with multilinear elements for all the unknowns. Due to the high convective effects we need to stabilize the formulation by some special technique

like SUPG (“*Streamline Upwind - Petrov Galerkin*”, otherwise spurious oscillations are frequently encountered. Once the spatial discretization is performed the partial differential system of equations is transformed into an ordinary differential system of equations like:

$$\dot{U} = R(U) \quad (34)$$

where U is the state vector containing the three unknowns in each node of the whole mesh. So, the system dimension is $3N$ where N is the number of nodes in the mesh. The numerical procedure is as follow: Knowing the state vector at the current time (t^n), i.e. $U_j(t^n) = [T_j, H_j, \rho_{a,j}](t^n)$ where j represent an specific node in the mesh. To get the residual, right hand side of equation 34 the following steps should be done:

- From the gas state equation $(T, \rho_a) \rightarrow P_a$,
- From soption isotherms $(T, H) \rightarrow HR \rightarrow P_v$,
- From vapor state equation $(T, \rho_v) \rightarrow P_v$,
- Compute some state dependent coefficients from additional constitutive laws, like $\rightarrow D^*, K_g, k_{x,y}, C_p$, and so on ...
- Compute gradients of T, P , so on... at some specific Gauss points in each element of the mesh.
- Compute each element residual contribution and gather in a global vector

Once the whole residual vector at $t = t^n$ is computed the unknowns variables at the next time step is updated from the following equation:

$$U^{n+1} = U^n + \Delta t R(U^n) \quad (35)$$

This kind of scheme, called *explicit integration in time* is very simple to be implemented but it has two major drawbacks, one is the limitation of the time step to ensure numerical stability and the other is the bad convergence rate for ill-conditioned system of equations. In this application the last disadvantage is very restrictive because the characteristic times of each equation are very different. To circumvent this drawback we have implemented an implicit numerical scheme like:

$$U^{n+1} - \Delta t R(U^{n+1}) = U^n \quad (36)$$

where the residue is computed at the new state variable $U(t^{n+1})$ instead of using the current value $U(t^n)$. The non-linearities and the time dependency of the state vector makes this implementation more difficult and time consuming but more stable. Due to the non-linearities a Newton-Raphson method is highly recommended being the jacobian computation one of the more difficult problems to be done specially for this application where the coefficients of the balance equations have a strong dependency with the state vector. In order to get a robust code we adopt a numerical computation of the jacobians,

$$J = \frac{\partial R}{\partial U} \quad (37)$$

using a finite difference method like:

$$J \approx J_{num} = \frac{R(U + \delta U) - R(U)}{\delta U} \quad (38)$$

If we performe this strategy in an elementwise form the cost involved is $O(N)$. In our application and despite of the ill-condition of the problem we have found a good convergence at each time step, in average 4 iterations per time step to reduce 10 orders of magnitude in the global residue.

4 Physical and transport properties

4.1 Thermal conductivity

Following Humphrey [4] the influence of board density, moisture content and temperature on the thermal conductivity is considered once at each time. The effect of each variable is defined as a factor upon the main definition:

$$\kappa_z = 1.172 \times 10^{-2} + 1.319^{-4} \rho_s \quad (39)$$

where κ_z is the thermal conductivity in the pressing direction in $W/m/K$ and ρ_s is the oven dry density of the material in Kg/m^3 . Considering the basal or reference value as:

$$\kappa_z = 0.09 W/m/K \quad \text{for } \rho_s = 650 Kg/m^3 \quad (40)$$

4.1.1 Density correction

$$F_{\kappa,\rho} = (\rho_s - 586) \times 1.46 \times 10^{-3} + 1 \quad (41)$$

4.1.2 Moisture correction

From Kollmann and Malmquist (1956) and Humphrey (1982)

$$F_{\kappa,H} = (H - 12) \times 9.77 \times 10^{-3} + 1 \quad (42)$$

with H the moisture content of the board material in %

4.1.3 Temperature correction

From Kuhlmann (1962) and Humphrey (1982)

$$F_{\kappa,T} = (T - 20) \times 1.077 \times 10^{-3} + 1 \quad (43)$$

with T in Celsius degrees.

4.1.4 Heat flux direction correction

By far the greater part of conductive heat translation takes place in the vertical plane. However the energy lost from the mattress is largely the result of radial vapour migration from the centre towards the atmosphere. The associated horizontal relative humidity gradient lead to a horizontal temperature gradient. Even though this gradient is always lower than the vertical one its influence should be taken into account if multidimensional analysis is required. Following the few Ward and Skaar laboratory measurements (1963) they observed that at a first glance a factor of approximately 1.5 may be a good initial guess before doing some extra measurements. Then

$$\kappa_{xy} = 1.5\kappa_z \quad (44)$$

4.2 Permeability

The evaporation and condensation of water changes the vapour density and consequently its partial pressure in the voids within the composite. A vertical pressure gradient leads to the flow of water vapour from the press platens towards the central plane of the board. At the same time an horizontal vapour flow is set up in response to the pressure gradient established in the same direction. The relation between the pressure gradient and the flow features may be assigned to the material permeability. Permeability is a measure of the ease with which a fluid may flow through a porous medium under the influence of a given pressure gradient. Different mechanisms may be involved in this flow, a viscous laminar flow, a turbulent flow and a slip or Knudsen flow. In this study only the first type is included with the assumption that Darcy law is obeyed. This hypothesis should be verified experimentally. However for our preliminar work we have assumed it. This may be written as:

$$\nabla p = -\frac{\mu_g}{K_g} \mathbf{v}_g \quad (45)$$

where ∇p is the driving force and \mathbf{v}_g is the flow variable. $\frac{K_g}{\mu_g}$ is called the superficial permeability with μ_g the dynamic viscosity of the gas phase and K_g the specific permeability. When Darcy law is applied to gaseous flow the compressibility of the fluid should be taken into account. Humphrey suggested to use a correction factor for the superficial permeability as:

$$\frac{K_g}{\mu_g} \frac{\bar{P}}{P} \quad (46)$$

where \bar{P} is the mean pressure value along the flow path and P is the local total pressure.

Relative to the viscosity the kinetic theory of gases suggests that at normal pressure the viscosity is independent of pressure and it varies as the square root of the absolute temperature,

$$\mu \propto \sqrt{T} \quad 10^3 < p < 10^6 \quad (47)$$

Corrections with the absolute temperature are often considered by Sutherland law:

$$\mu = \frac{B T^{3/2}}{T + C} \quad (48)$$

with B and C characteristic constants of the gas or vapour with μ in $Kg m^{-1} s^{-1}$. Values for B and C are available from Keenan and Keyes (1966). For this application the following expression was adopted:

$$\mu = 1.112 \times 10^{-5} \times \frac{(T + 273.15)^{1.5}}{(T + 3211.0)} \quad (49)$$

with T in $^{\circ}C$.

4.2.1 Variation of vertical permeability with board material density

Even though we consider that the press is closed and the density profile is set up and fixed it is included here some conclusions from Humphrey thesis with results obtained by Denisov (1975) for 19 mm boards and others from Sokunbi (1978). The data to be fitted are the following:

Table I: Vertical permeability density correction data

	Mean density Kg/m^3	Mean vertical permeability $m^2 \times 10^{15}$
	425	64
	475	40
	525	24
	575	16
	625	11
	675	7
	725	5
	775	3
	825	2
	875	2

4.2.2 Horizontal permeability

Sokunbi measures included in figure 2.7 of Humphrey thesis shows the relation between the board thickness in mm with horizontal permeability. For approximately $15mm$ board thickness and $\rho_s \approx 650Kg/m^3$ we have that the horizontal permeability is 100 the vertical value. However, if using $586Kg/m^3$ for the oven dry material instead we have a factor of 59 that agrees with that reported by Carvalho-Costa .

4.3 Vapour Density

For the pressure range likely to occur during hot pressing (between 10^3 and 3×10^5) a linear relationship between saturated vapour pressure and vapour density may be assumed. Fitting experimental data Humphrey had proposed the following expression:

$$\rho_v = P_{sat} \times 6.0 \times 10^{-8} \times HR \quad (50)$$

with ρ_v in Kg/m^3 , P_{sat} in N/m^2 and the relative humidity HR in %. By definition

$$HR = P_v / P_{sat} \quad (51)$$

and applying ideal gas law for gaseous phase

$$\frac{P_v}{\rho_v} = \bar{R} / M_w T \quad (52)$$

Taking $\bar{R} = 8314J/Kmol/K$ and $M_w = 18Kg/Kmol$ with $T \approx 400K$ we may get the 6.0×10^{-8} factor in 50

4.4 Saturated vapour pressure

Following the Kirchoff expression with data presented by Keenan and Keys (1966) we include here the following equation:

$$\log_{10} P_{sat} = 10.745 - (2141.0 / (T + 273.15)) \quad (53)$$

with P_{sat} in N/m^2 and T in $^{\circ}C$.

4.5 Latent heat of evaporation and heat of wetting

Using Clausius-Clapeyron equation in differential form and after some simplification the latent heat of vaporization of free water may be written as:

$$\lambda = 2.511 \times 10^6 - (2.48 \times 10^3 \times T) \quad (54)$$

with λ in J/Kg and T in $^{\circ}C$.

For the differential heat of sorption we follow Humphrey that used Bramhall (1979) expresion:

$$Q_l = 1.176 \times 10^6 \times \exp(-0.15H) \quad (55)$$

with Q_l in J/Kg and H in %.

4.6 Specific heat of mattress material

It is computed by adding the specific heat of dry wood and that of water according to the material porosity and assuming full saturation. The specific heat of dry mattress material is taken as $1357K/Kg/K$ and the specific heat of water has been taken to be $4190J/Kg/K$. From Siau (1984) the expression for specific heat of moist wood is:

$$C_p = 4180 \frac{0.268 + 0.0011(T - 273.15) + H}{1 + H} \quad (56)$$

4.7 Porosity

According to Humphrey the volume of voids within the region may be computed by

$$\epsilon = \frac{V_{voids}}{V} = (1 - \frac{\rho}{\rho_s}) \quad (57)$$

where ϵ is the porosity, ρ is the density of the region and ρ_s is the dry density of the board material.

In Carvalho-Costa paper they included the expression from Suzuki and Kato (1989):

$$\epsilon = 1 - \rho_s \frac{1/\rho_f + y_r/\rho_r}{1 + y_r} \quad (58)$$

where ρ_r is the cure resin density, ρ_f is the oven dry fiber density and y_r is the resin content (resin weight/board weight). In its paper Carvalho-Costa had used $y_r = 8.5\%$ with $\rho_f = 900Kg/m^3$ and $\rho_r = 1100Kg/m^3$.

5 Numerical results

In this section we present some results obtained from Humphrey PhD. thesis. This numerical experiment allows the validation of the mathematical model and its numerical implementation for future applications to hot-pressing process simulation and control. This experiment consists of an round fiberboard of 15 mm of thickness and 0.2828 m of radius that according to its axisymmetrical geometry needs as spatial

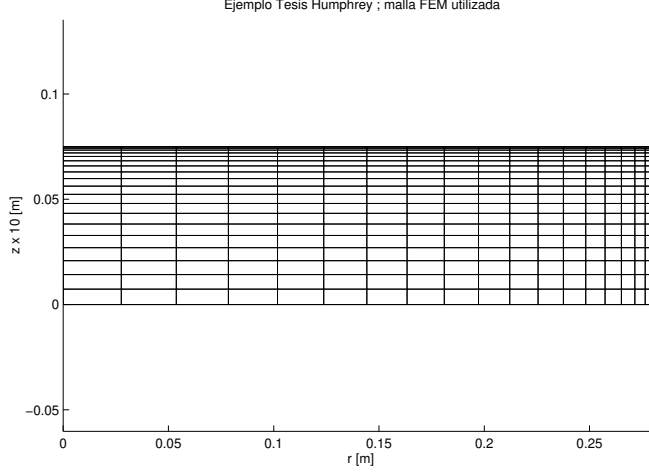


Figure 1: Finite element mesh

coordinates only the radius r and the axial coordinate z assuming no variation in the circumferencial coordinate. The axisymmetrical domain is discretized in 20×20 elements in each direction with a grading towards the press platen and the external radius as may be visualized in figure 1. In order to follow the same assumptions as Prof. Humphrey we have fixed the air to a very low value ($\rho_a \approx 10^{-6}$) because he had assumed that the press was close with no air inside the fiberboard.

We have adopted the following boundary conditions:

- thermally adiabatic at $r = 0$, at $z = 0$ and at $r = R_{ext} = 0.2828m$
- temperature at $z = 15mm/2$ fixed to follow the time evolution of press platen temperature $T_{press} = T(t)$
- moisture transfer isolated at $z = 0, z = 15mm/2$ and $r = 0$
- We experienced with two possibilities for the vapour pressure boundary condition at the external radius $r = R_{ext} = 0.2828m$:

$$p_v(r = R_{ext}) = HR_{atm}P_{sat}(T_{atm}) \quad (59)$$

For the press platen temperature we have applied a ramp from 30° at $t = 0$ to 160° at $t = 72$ seconds with a least square fitting from Humphrey data. As initial conditions we have assumed a uniform temperature of $T(t = 0) = 30^\circ$ in the whole solid material with a uniform moisture content of $H = 11\%$.

In the next section we include the results obtained by using the model above cited to the original problem presented by Humphrey. Next we present some other experiments showing some phenomena that deserve more attention for future studies.

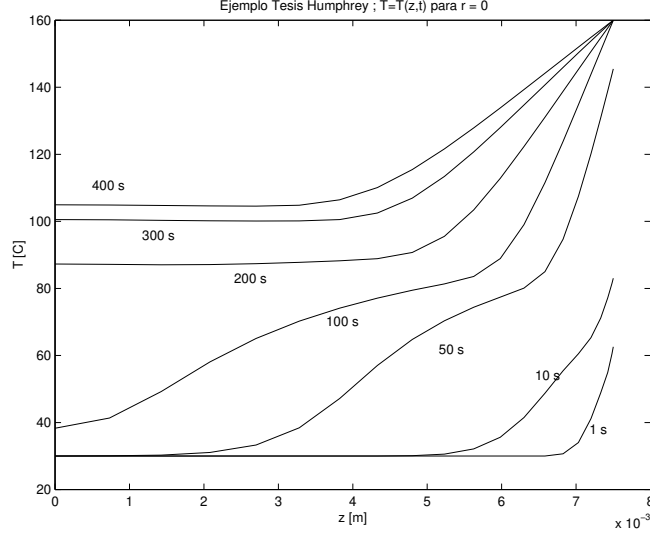


Figure 2: Axial temperature profile at $r = 0$

5.1 Original numerical experiment

Figure 2 shows the temperature distribution in time and with the axial coordinate at $r = 0$ (centerline). We can note the penetration in the axial direction of the temperature profile in time for $t = 1, 10, 50, 100, 200, 300$ and 400 seconds. Figure 3 shows the same kind of plot for moisture content.

The following figures show similar plots but at different locations,

- 4 : temperature at external radius
- 5 : moisture content at external radius
- 6 : temperature at axial centerline ($z = 0$)
- 7 : moisture content at axial centerline ($z = 0$)
- 8 : moisture content at press platen

The radial temperature profile at press platen is not shown because its distribution is fixed as input data.

Figure 9 shows several isotherms at $t = 200$ seconds distributed in the r, z plane.

Figure 10 shows a three-dimensional view for moisture content represented by the third coordinate axis at $t = 200$ seconds as a function of r, z .

These results are in good agreement with those presented by Humphrey in his thesis. However the cited author did not present his results at some locations that in our opinion should be treated with some care, for example at the external radius.

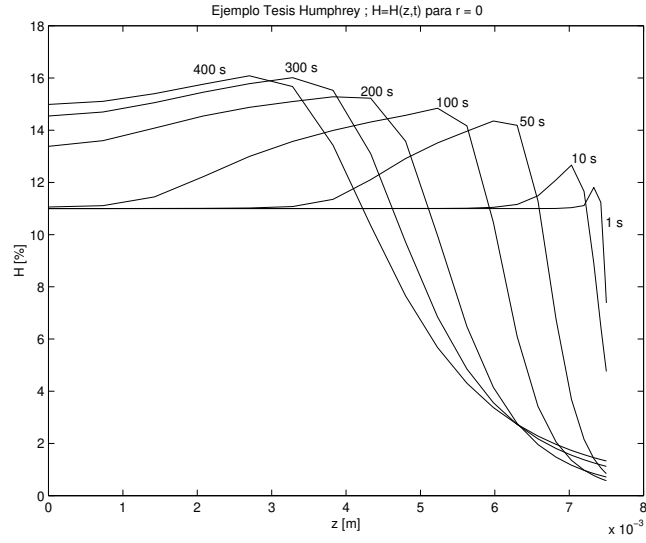


Figure 3: Axial moisture content profile at $r = 0$

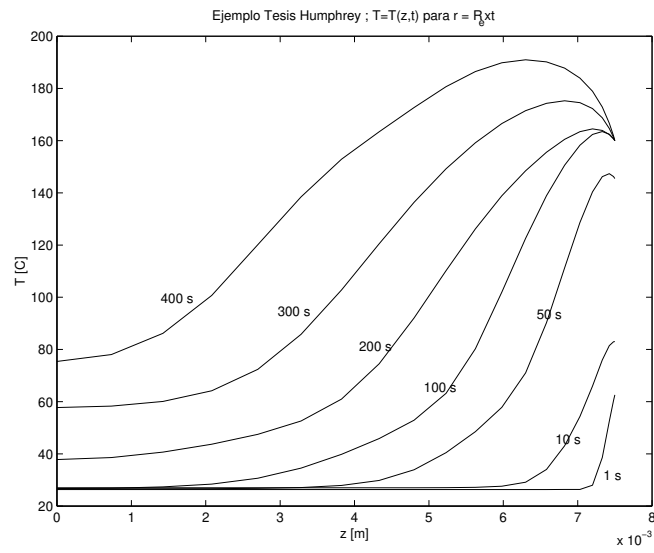


Figure 4: Axial temperature profile at $r = R = 0.2828m$

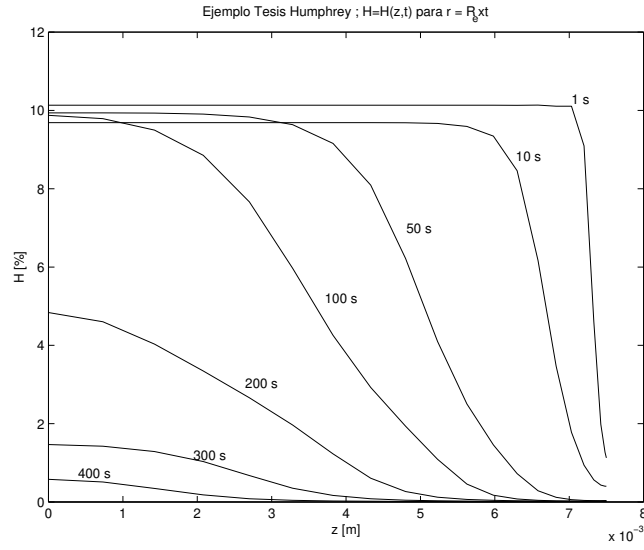


Figure 5: Axial moisture content profile at $r = R = 0.2828m$

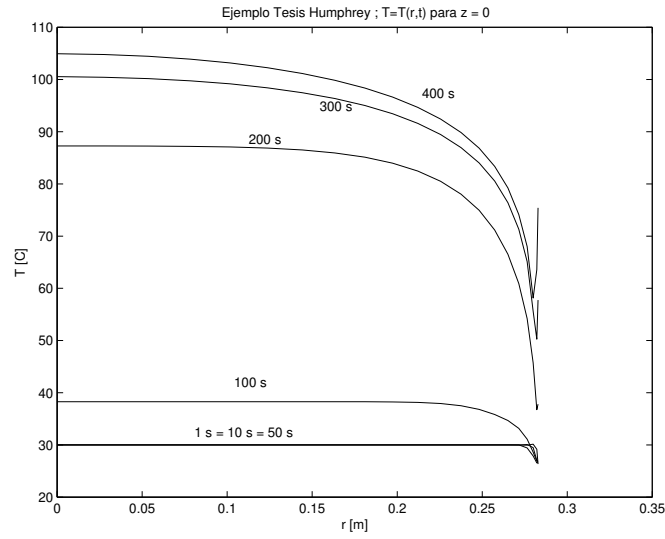


Figure 6: Radial temperature profile at $z = 0$

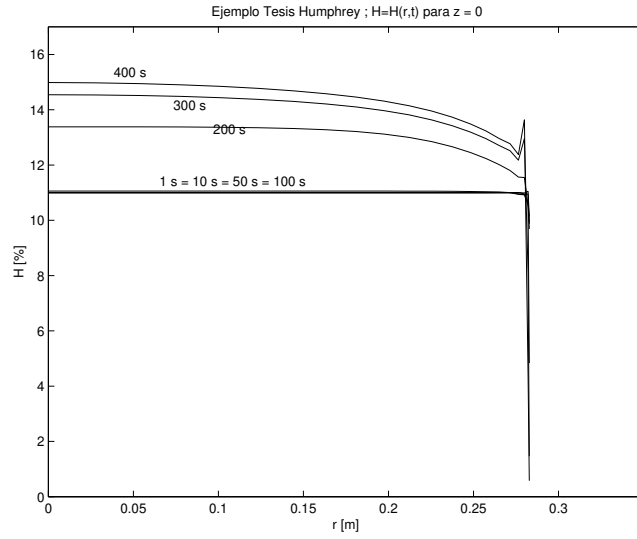


Figure 7: Radial moisture content profile at $z = 0$

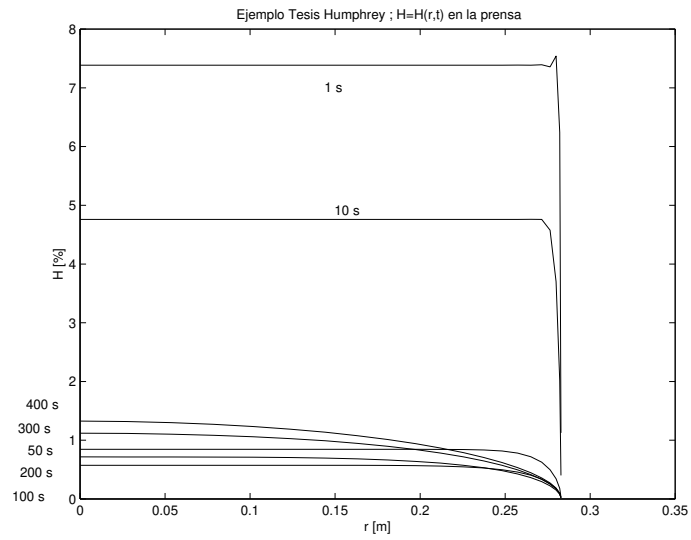


Figure 8: Radial moisture content profile at press platen

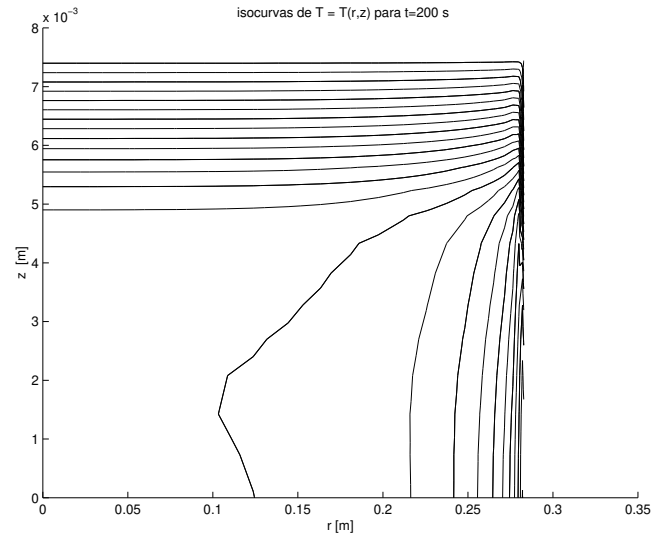


Figure 9: Isotherms at $t=200$ seconds

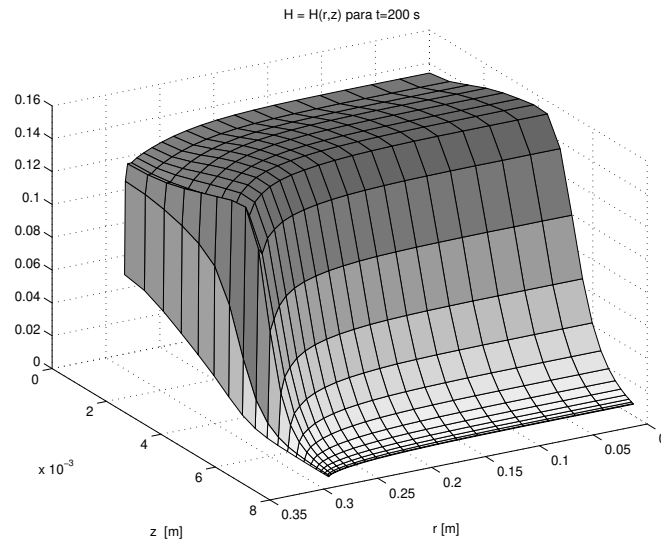


Figure 10: 3D view for moisture content at $t=200$ seconds

5.2 Further numerical experiments

Humphrey only include results for moisture and temperature in the vertical and radial directions at both central planes, $r = 0$ and $z = 0$ respectively. No mention about the vertical distribution at $r = R = 0.2828m$ or about the moisture content at press platen. Moreover, he had used a uniform mesh of 10×10 elements without showing what happen at the last annuli of elements corresponding to the external radius.

Our results present some overshooting in the temperature profile very close to the radial exit contour and at the first moment we thought about a spurious numerical problem, but it is due to large variations of the magnitude of vapour pressure and density at the boundary. In typical runs, vapour pressure varies from near 2 atm in the center of the board to 0.01 atm at the external radius. We think that this problem will be fixed if we solve for the air density also, but then a very fine grid will be necessary at the exit boundary, since large variations of the vapour molar fraction are expected. (see 11). Molar fraction varies from nearly 1 at the interior of the mat to a 2% at the external atmosphere. This variation is produced in a thin layer of width δ proportional to the diffusivity of vapour in air which is very small.

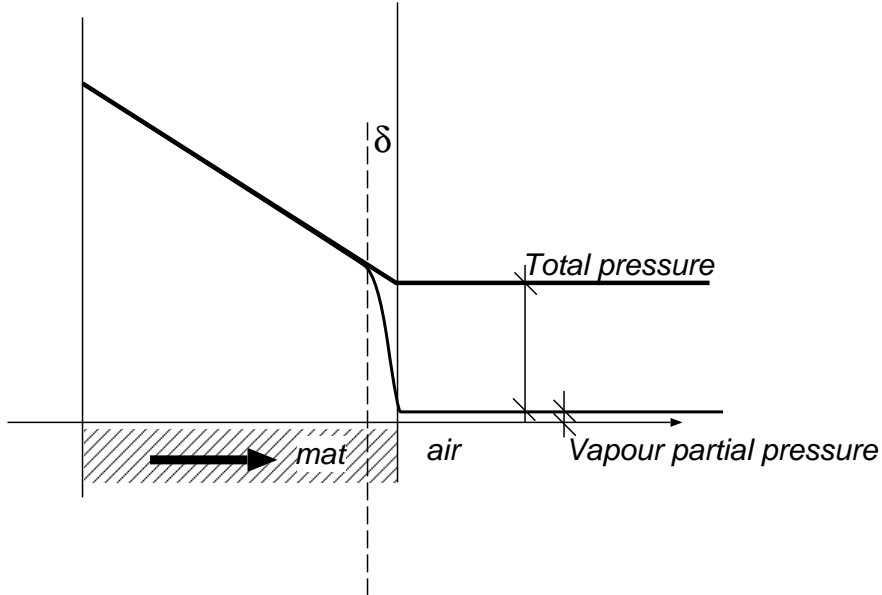


Figure 11: CAPTION

6 Appendix. Derivation of the averaged energy balance equation

The microscopic energy balance equation in the gas phase is

$$\frac{\partial}{\partial t}(\rho h) + \nabla \cdot (\rho \mathbf{v} h) = -\nabla \cdot (k \nabla T) \quad (60)$$

For the other phases (solid and bound water) a similar expression holds, but neglecting the advective term. Applying the volume average operator[14], we arrive to the following equation averaged on the gas phase:

$$\frac{\partial}{\partial t}(\epsilon_g \langle \rho h \rangle^g) + \nabla \cdot (\epsilon_g \langle \rho h \mathbf{v} \rangle^g) = \nabla \cdot (\epsilon_g \langle k \nabla T \rangle^g) + Q_g \quad (61)$$

ϵ_g is the volumetric fraction of phase g (i.e. gas) and $\langle X \rangle^g$ is the average of quantity X on the volume occupied by phase g

$$\langle X \rangle^g = \frac{1}{\Omega_g} \int_{\Omega_g} X \, d\Omega \quad (62)$$

The term Q_g is the total enthalpy flux through the solid-gas interface Γ

$$Q_g = \int_{\Gamma} (\rho h)_g (\mathbf{v} - \mathbf{w}) \cdot \hat{\mathbf{n}} \, d\Gamma \quad (63)$$

where $(X)_g$ is the value of property X on the g side of the interface and \mathbf{w} is the velocity of the interface. Assuming that h_g is constant on all Ω_g (for a certain volume control) then

$$Q_g = \langle h \rangle^g \int_{\Gamma} (\rho)_g (\mathbf{v} - \mathbf{w}) \cdot \hat{\mathbf{n}} \, d\Gamma \quad (64)$$

$$= \langle h \rangle^g \dot{m} \quad (65)$$

where \dot{m} is the rate of mass of water being evaporated. A common drawback of averaged equations is that, when products of variables like ρh appear in the microscopic equation, the average of the product $\langle \rho h \rangle^g$ is obtained in the averaged equation. Now, it is not true that

$$\langle \rho h \rangle^g = \langle \rho \rangle^g \langle h \rangle^g \quad (66)$$

so that the averaged equation contains more unknowns than the original equation. A common assumption is to assume that no correlation exists between variables and so (66) is approximately valid.

Then, applying the volume average operator over the gas, solid, and bound water phases and assuming no correlations between variables we obtain the following averaged equations for the three phases:

$$\frac{\partial}{\partial t}(\epsilon_g \rho_g h_g) + \nabla \cdot (\epsilon_g \rho_g \mathbf{v}_g h_g) = \nabla \cdot (\epsilon_g \langle k \nabla T \rangle^g) - \dot{m} h_g \quad \text{gas phase} \quad (67)$$

$$\frac{\partial}{\partial t}(\epsilon_s \rho_s h_s) = \nabla \cdot (\epsilon_s \langle k \nabla T \rangle^s) \quad \text{solid phase} \quad (68)$$

$$\frac{\partial}{\partial t}(\epsilon_l \rho_l h_l) = \dot{m} h_l \quad \text{liquid phase} \quad (69)$$

Now, summation of these three equations gives:

$$\frac{\partial}{\partial t}(\epsilon_g \rho_g h_g + \epsilon_s \rho_s h_s + \epsilon_l \rho_l h_l) + \nabla \cdot (\epsilon_g \mathbf{v}_g \rho_g h_g) = \nabla(\epsilon_g \langle k \nabla T \rangle^g + \epsilon_s \langle k \nabla T \rangle^s) + \dot{m}(h_l - h_g) \quad (70)$$

Now,

$$\epsilon_g \langle k \nabla T \rangle^g + \epsilon_s \langle k \nabla T \rangle^s = k_{\text{eff}} \nabla \langle T \rangle \quad (71)$$

where k_{eff} is the average conductivity of the solid+water+gas mixture. The gas is assumed as an ideal mixture, so that the enthalpy is the sum of the enthalpy of its constituents, and neglect the contribution of the air constituent so that

$$\rho_g h_g = \rho_a h_a + \rho_v h_v \approx \rho_v h_v \quad (72)$$

Taking a reference state for the enthalpy at a point on the adsorbed state

$$h_v = C_{pv}(T - T_{\text{ref}}) + \lambda + Q_l \quad (73)$$

We also neglect the enthalpy of the gas phase with respect to the solid+water phases and put

$$\epsilon_s \rho_s h_s + \epsilon_l \rho_l h_l = (\rho C_p)_{\text{eff}} (T - T_{\text{ref}}) \quad (74)$$

where ρ_{eff} , and $C_{p\text{eff}}$ are averaged properties for the moist board, as a function of temperature and moisture content. Finally, the averaged equation is

$$\frac{\partial}{\partial t}[(\rho C_p)_{\text{eff}} (T - T_{\text{ref}})] + \nabla \cdot [\epsilon_g \rho_v \mathbf{v}_g (C_{pv}(T - T_{\text{ref}}) + \lambda + Q_l)] = \nabla \cdot (k_{\text{eff}} T) - \dot{m}(\lambda + Q_l) \quad (75)$$

References

- [1] G. Bramhall. Mathematical model for lumber drying. i. principles involved. *Wood Sciences and Technology*, 12(1):14–21, 1979.
- [2] L.M.H. Carvalho and C.A.V. Costa. Modeling and simulation of the hot-pressing process in the production of medium density fiberboard (mdf). *Chem. Eng. Comm.*, 170 1–21, 1998.
- [3] O. B. Denisov, P.P. Anisov, and P.E. Zuban. Untersuchung der permeabilitat von spanfliesen. *Holztechnologie*, 16(1):10–14, 1975.
- [4] P. Humphrey. *Physical aspects of wood particleboard manufacture*. PhD thesis, Univ. of Wales, U.K., 1982.
- [5] P. Humphrey and A. Bolton. The hot pressing of dry-formed wood-based composites. part ii. a simulation model for heat and moisture transfer, and typical results. *Holzforschung*, 43:199–206, 1989.

- [6] J. Keenan and F. Keyes. *Thermodynamic properties of steam*. John Wiley and Sons., London, 1966.
- [7] F. Kollmann and Malmquist L. Über die wärmeleitzahl von holz und holzwerkstoffen. *Holz Roh-Werkstoff*, 14(16):201–204, 1956.
- [8] G. Kuhlmann. Untersuchung der termischen eigenschaften von holz und spanplatten in abhängigkeit von feuchtogkeit und temperatur im hygroskopischen bereich. *Holz Roh-Werkstoff*, 20(7):259–270, 1962.
- [9] P. Kuts and N. Grinchik. Two-phase filtration equations and sorption isotherms as applied for studying kinetics and dynamics of drying process. In A. Mujumdar, editor, *Proc. Drying of solids. Recent International developments*, 1986.
- [10] J. Liu, S. Avramidis, and S. Ellis. Simulation of heat and moisture transfer in wood during drying under constant ambient conditions. *Holzforschung*, 48:236–240, 1994.
- [11] O.K. Sokunbi. Aspects of particleboard permeability. Master’s thesis, University of Wales, U.K., 1978.
- [12] M. Suzuki and T. Kato. Influence of dependent variables on the properties of mdf. *Mokuzai Gakkaishi*, 35(1):8, 1989.
- [13] R. Ward and C. Skaar. Specific heat and conductivity of particleboard as a function of temperature. *For. Prod. J.*, 13(1):32, 1963.
- [14] S. Whitaker. Heat and mass transfer in granular porous media. In A.S. Mujumdar, editor, *Advances in Drying*, volume 1, pages 23–61. McGraw Hill, Hemisphere P.C., Washington, 1980.